

## Research Paper

## Composition analysis of natural gas in the presence of liquid impurities by high-pressure proton low-field Nuclear Magnetic Resonance spectroscopy

S.A. Ortiz Restrepo<sup>a</sup>, J. Denninger<sup>a</sup>, P.M. Dupuy<sup>b</sup>, H.C. Widerøe<sup>b</sup>, O. Mohnke<sup>c</sup>, Ø. Leknes<sup>d</sup>, A. Adams<sup>a,\*</sup><sup>a</sup> Institut für Technische und Makromolekulare Chemie, RWTH Aachen University, Templergraben 55, 52056 Aachen, Germany<sup>b</sup> Equinor ASA, Arkitekt Ebbells veg 10, 7053 Ranheim, Norway<sup>c</sup> Baker Hughes INTEQ GmbH, Baker Hughes Strasse 1, 29221 Celle, Germany<sup>d</sup> Gassco AS, Bygnesvegen 75, 4250 Kopervik, Norway

## ARTICLE INFO

## Keywords:

Natural gas quantification  
Nuclear Magnetic Resonance  
High pressure  
Indirect Hard Modelling  
Triethylene glycol  
Gas dehydration

## ABSTRACT

Natural gas (NG) plays a key role in the transition to greener energy sources. Accurate composition analysis is essential for determining NG's commercial value and ensuring efficiency across the entire value chain. Since NG typically contains water, it is dehydrated using agents like triethylene glycol (TEG). However, residual liquid TEG may remain in the pipeline, compromising sample quality for conventional NG composition analysis, which can measure only the gaseous phase. Thus, this work demonstrates the applicability of high-pressure (HP) benchtop <sup>1</sup>H NMR spectroscopy for analyzing wet NG, with the simultaneous detection of gas and liquid phases. To enhance the robustness of the method, additional quality control parameters (QC) for the NMR signal were implemented alongside with previously established QCs. The methodology was validated using a three-component NG sample at 200 bar, in the presence of TEG as dynamic droplets and at varying stationary amounts within the sensitive volume. The determined NG composition was in excellent agreement with the vendor certificate. Moreover, the detection and quantification limits of TEG under the employed experimental conditions were determined. This work represents a significant step towards the integration of HP benchtop NMR spectroscopy for real-time monitoring of wet NG composition in industrial environments.

## 1. Introduction

Natural gas (NG) is nowadays an important source of energy worldwide covering 28 % of the total energy demand in 2024 [1]. Its global consumption reached an all-time high in the same year [2]. NG is crucial in various fields of activities including the industrial, residential, and electricity sectors [3]. With the continuously increase in the global energy demand and the accompanied greenhouse effect, NG has been promoted as a “bridge” fuel in the transition towards a decarbonized energy sector [4,5]. As an example, NG produces emissions less than about half of emissions produced by coal [4]. Moreover, it is expected that NG will have a similar role at least until 2040 [6] and most probably also later on.

In the context of continuous changing demographical, political, and economical situation, the knowledge of the NG prices is very important not only for the energy policy but also for an improved management of the energy resources [7]. The price is determined by its composition,

which can vary from production to production site and along the distribution network [7,8].

Usually, the natural gas contains large amounts of water. Due to the demand of meeting specific sale specifications, a gas dehydration process is used in the natural gas industry to remove the water [9,10]. Dehydration is an important step for maintaining the water content under a certain threshold. This is because the water can cause pipeline corrosion which can be detrimental for its integrity. Moreover, it can lead to the formation of hydrates which impact the efficiency of the gas transmission through the pipeline [11].

Various solid and liquid samples have been proposed to remove the water from the NG [12] with the glycols being so far the most efficient [13–16]. The general formula of these simple chemical compounds containing two hydroxyl groups (–OH) can be described as HO–(CH<sub>2</sub>–CH<sub>2</sub>O)<sub>n</sub>–H. Among glycols, triethylene glycol (TEG) with *n* = 3 is the most popular dehydration agent implemented in natural gas streams due to its chemical stability, lower cost, and its high affinity to water,

\* Corresponding author.

E-mail address: [Alina.Adams@itmc.rwth-aachen.de](mailto:Alina.Adams@itmc.rwth-aachen.de) (A. Adams).<https://doi.org/10.1016/j.enconman.2025.120258>

Received 11 February 2025; Received in revised form 11 July 2025; Accepted 18 July 2025

Available online 25 July 2025

0196-8904/© 2025 The Authors. Published by Elsevier Ltd. This is an open access article under the CC BY license (<http://creativecommons.org/licenses/by/4.0/>).

attributed to complex intermolecular interactions through H-bonds between the OH group and the H<sub>2</sub>O molecules [17]. To increase the efficiency of the drying process at reduced operational costs, a quantification of the amount of dehydration compounds such as TEG or mono-ethylene glycol (MEG) or mixtures of them with the help of appropriate analytical methods would be needed. So far, Fourier Transform Infrared (FTIR) spectroscopy and NMR have been proposed for the quantification of such liquid mixtures [18,19] but, to the best of our knowledge, never in the presence of a NG sample pressurized at relevant industrial pressures.

Moreover, in downstream in-field applications where processing units such as dehydration units, separators, and scrubbers exist, the gas stream is directed through a conditioning system to lower the hydrocarbon (HC) dew point to levels suitable for transport, injection, or sales gas specifications [20]. Thus, the dry natural gas can be contaminated with liquid TEG either through direct carryover from the dehydration unit or through condensation following TEG evaporation at elevated inlet gas temperatures [10]. In both cases, TEG is introduced into the gas stream as liquid droplets, which may coalesce over time and form accumulations [10,21].

Gas chromatography (GC) is nowadays the gold standard for the composition analysis of natural gas as it delivers high quality results along with very low limits of detection (LOD) and limits of quantification (LOQ) [22]. Yet, the method requires a carrier gas and the measurements need to be conducted at atmospheric pressures [23–25]. In addition, GC can deliver reliable results only for gaseous samples. According to international standards such as ISO TR 14749 [26] and ISO 10715 [21], it is explicitly required that liquid contaminants (e.g., water and glycols) have been effectively removed to prevent analytical errors, GC failure, and other operational issues. Additionally, sampling accessories for the liquid elimination systems are recommended to undergo regular maintenance. Moreover, the use of multiple calibration standards is necessary to ensure accurate measurements. Significant errors can occur, particularly when the sample composition differs from the standard's concentration [24]. Additionally, factors such as the injected sample volume, the concentration range of the calibration standards, and the linearity of the detector response critically influence the accuracy of GC predictions [23]. Therefore, GC measurements are conducted under well-controlled conditions.

Currently, there is a huge research effort towards the establishment of alternative methods to the GC. Especially optical spectroscopic methods such as infrared (IR) and Raman spectroscopy have a high potential for the composition analysis of natural gas, with most scientific research concentrating on investigating dry natural gas samples [27–37].

According to ISO 23978, even for Raman spectroscopy applied for the quantitative determination of chemical composition of natural gas in upstream area, the measurements should be conducted on homogeneous samples fully in the gas phase [35]. In addition, regular calibration of the equipment is required using standard gas mixtures that contain appropriate concentrations and cover the range of samples to be analyzed.

Only very few studies address the situation where water is present as vapor in the natural gas [29,32]. For example, Ref. [29] has recently demonstrated the successful use of near-infrared (NIR) spectroscopy combined with extensive chemometric modeling to quantify natural gas composition under water-saturated conditions. For this, liquid water was added as a thin water layer in the high-pressure cell to ensure the water saturation of the gas phase. The NIR measurements themselves have been carried out only in the gaseous phase containing the gaseous water and by avoiding the direct contact of the NIR probe with the liquid water.

Up to now and to the best of our knowledge, no reports exist about the application of these methods for the composition analysis of natural gas in the presence of liquid impurities (ex. water or glycol) with simultaneous information about the composition of the gas phase and

the detection and quantification of the liquid phase. In addition, the application of these methods under real conditions is also challenged by various factors including the pressure and temperature dependence of the signals to be used for the quantification purpose [36]. Furthermore, it is known that infrared spectroscopy is extremely sensitive to the presence of water, even in trace amounts. As for example, in the near IR (NIR) region which is proposed to be used for the composition quantification of natural gas, water shows a strong absorption band, which raises difficulties in the spectra analysis [37]. In the case of Raman spectroscopy, the rather weak scattering efficiency of water molecules compromises the accuracy of their quantification based on spectral features [33,34]. Furthermore, for Raman spectroscopy is pointed out that the dispersion of the laser beam caused by liquid droplets, such as water or heavy hydrocarbons, can lead to high noise levels in the recorded spectra affecting the accuracy of the composition analysis. In addition, condensate on the window cell may cause window damage and reduction of the optical transmission performance [31,32,38]. In the worst case scenario, only the condensate sticking on the window cell will be detected while the gas phase behind it will be invisible. Furthermore, it is reported that for gas/liquid mixtures, both optical methods are highly sensitive to the homogeneity of the sample. Thus, for reliable results, the measurements need to be conducted on a homogenous mixture. For this purpose, stirring devices are usually employed [39,40]. Using a purpose-designed experimental setup to ensure a homogeneous mixture is not an obstacle for analyses conducted under laboratory conditions; however, it can potentially be disadvantageous for in-field analyses. Most likely, for the mixtures investigated within the frame of the current study, the presence of liquid glycols in the natural gas will lead to a heterogeneous liquid/gas mixture and thus their analysis by optical methods will be far from being trivial. Thus, the identification and implementation of more versatile and low-cost analytical methods is highly necessary.

Nuclear Magnetic Resonance (NMR) spectroscopy represents another powerful alternative to the GC method and it is a well-accepted analytical tool for the analysis of complex mixtures [41–43]. Its key advantage is its quantitative principle, as the integral of a particular signal is directly proportional to the number of nuclei contributing to it and, consequently, to the amount of sample. NMR spectroscopy is highly effective for analyzing mixtures that exist in a single homogeneous phase, such as liquid or gas phase. In contrast, NMR spectroscopic analysis of mixtures containing separated phases (ex. liquid–liquid, liquid–gas) is challenging due to the differing magnetic environments and interfaces between phases, which can lead to broadened, overlapping, and distorted signals. Thus, only very few studies address the composition quantification of such samples using NMR spectroscopy [43,44]. These investigations concern samples containing two immiscible phases (liquid–liquid and gas–liquid) with one phase on the top of the other phase. The sample is inside a vertical NMR tube and placed inside the NMR spectrometer. Each phase is then selectively analyzed by shifting the position of the NMR tube inside the spectrometer such that only one phase is inside the sensitive volume during the measurement [43,44]. While this approach is applicable in a laboratory and only for samples having a horizontal separation between the two phases, it fails to be applied under online conditions where both phases can be present inside the detection region of the NMR spectrometer.

Very recently, high-pressure (HP) proton low-field NMR spectroscopy has been introduced as a new analytical method for the composition analysis of dry natural gas [45]. It took advantage of a novel high-pressure setup designed for low-field NMR spectroscopy, which enabled the measurement of gaseous samples up to 200 bar [46]. Given that each investigated HC within the natural gas has unique signatures in the proton NMR spectra, the strong signal overlapping could be efficiently disentangled using indirect hard modelling (IHM). The determined compositions of various gaseous mixtures were in excellent agreement with the corresponding GC and vendor results.

In the current work, we demonstrate the applicability of the HP

proton low-field NMR spectroscopy for the composition quantification of pressurized wet natural gas containing liquid impurities with exemplification on aqueous TEG. Given the before mentioned issues with the measurement of immiscible samples, the performance of the NMR method was tested in the first step on gas samples containing various TEG amounts under static conditions. In the second step, a dynamic condition was simulated with the help of a TEG droplet passing through the sensitive volume during the conduction of the NMR measurements. It could be demonstrated that TEG amounts can be reliably quantified as low as 2.83 mg in the sensitive volume for both conditions, while the composition of the gaseous mixture can be determined in the presence of liquid TEG under static condition with amounts up to about 28.5 mg in the sensitive volume. The obtained values show an excellent agreement with the vendor certificate. Moreover, the LOD and LOQ of TEG present in the pressurized NG inside the sensitive volume of the NMR equipment could be determined. Based on the presented results, we expect HP NMR spectroscopy to be implemented in a wider range of applications where the quantitative analysis of pressurized gas samples can be challenged by the presence of liquid contaminants. This is particularly relevant for online composition monitoring under in-field scenarios where currently there are no analytical methods for composition analysis of natural gas containing liquid contaminants and where analytical instruments can't be continuously supervised.

## 2. Experimental section

### 2.1. Chemicals and materials

A gaseous mixture containing 85 % methane (C1), 10 % ethane (C2), and 5 % propane (C3) was purchased from Linde AG (Leuna, Germany). Its exact composition is given in Table S11. It was used as received. Molecular sieves of type 4 Å and triethylene glycol (CAS 112-27-6) with a purity of 99 % were purchased from Sigma-Aldrich. Distilled water used for preparing the glycol–water mixture was obtained from the facilities of the Institute for Technical and Macromolecular Chemistry (ITMC) at RWTH Aachen University.

### 2.2. High-pressure hardware for benchtop Nuclear Magnetic Resonance spectroscopy

The high-pressure setup depicted in Fig. 1 is suitable for benchtop

NMR spectroscopy and was built in ITMC, RWTH Aachen University. A detailed description of the experimental hardware is presented in our previous publications [46,47]. This work uses the refined high-pressure sapphire tube design (Fig. 1a) introduced in Ref. [47]. It has 5 mm outer diameter (o.d.), 3.4 mm inner diameter (i.d.), and a length of 178 mm. The gaseous sample is filled into one of the two chambers of a Prolight Ti 690-64 MB piston cylinder. These chambers are physically separated by an internal movable piston cylinder. The sample chamber can be connected either to the HP tube or to the sample bottle by turning a 3-way-valve and the final pressure sample can be adjusted by filling the second chamber with nitrogen gas. The maximum operating pressure is 206 bars. For pressures beyond this fixed limit, a safety spring valve releases the gas, keeping the operational safety and ensuring the mechanical integrity of the HP setup.

### 2.3. Sample preparation

To prepare an aqueous TEG sample with a controlled amount of water, TEG was previously stored for more than 4 months in a sample container with molecular sieves (previously activated at 600 °C for 8 h) under argon atmosphere at room temperature. Then, the residual water content in TEG after the storage was determined by the Karl-Fisher method. A final mixture of H<sub>2</sub>O-TEG with a water content of 22.5 wt% was prepared gravimetrically under an argon atmosphere. This water content in TEG was considered as a representative case among values reported in literature [19,48]. To minimize additional water uptake from the atmosphere, the H<sub>2</sub>O-TEG mixture was stored in a container with argon.

The mixture NG-TEG was prepared to mimic two in-field scenarios for the aqueous TEG in a NG pipeline. In the first scenario, the TEG was resting at the bottom of the sapphire tube as a stationary solution during the NMR measurements. In the second scenario, we considered a running droplet of the aqueous TEG solution while the NMR measurements of the NG-TEG sample were being conducted. For this, the HP tube was first hold in a horizontal position and a TEG droplet was placed with a syringe on the upper side of its inner wall (Fig. S11). For both scenarios, to minimize further water uptake from the atmosphere of the TEG solution, the inner volume of both the empty HP-tube and the syringe to handle the TEG sample were kept under an argon atmosphere during the sample preparation. Finally, with the TEG sample in place, the HP-tube was sealed with the PEEK attachment.



**Fig. 1.** Photograph of a) the HP sapphire tube proposed in Ref. [47] and b) the HP-setup and the employed benchtop NMR device introduced in Ref. [46], placed together inside a fume-hood.

To prepare the NG-TEG sample, the chamber sample side of the cylinder, the steel connecting capillaries, and the HP-tube were first evacuated for five minutes with a membrane pump. Subsequently, the bottle containing the gas sample was connected to the inlet sample attachment of the HP setup. After turning the 3-way-valve, the HP tube was isolated and the chamber sample side of the cylinder was connected to the sample-gas bottle and evacuated for five minutes. After the initial evacuation of the setup, all the steel capillaries, the chamber side of the piston cylinder, and the HP-tube containing the aqueous triethylene glycol, were flushed with the gas sample and evacuated again. This flushing and evacuating procedure was repeated three times to ensure that only the gas sample and the aqueous triethylene glycol were present in the HP-tube. Finally, the whole setup was filled with the gas sample at a pressure of 30 bar. The final pressure of about 200 bar was set by pressurizing with a nitrogen bottle the backpressure-side of the cylinder.

#### 2.4. Nuclear Magnetic Resonance experiments

The  $^1\text{H}$  NMR spectra were recorded with a Spinsolve 60 Ultra from Magritek (Aachen, Germany) working at a proton resonance frequency of 60 MHz and at an operation temperature of 26.5 °C. All spectra were acquired using a dwell-time of 200 microseconds and 32 k data points. A repetition time of 2 min between two consecutive scans was used to ensure quantitative data. This time is more than five times longer than the longest spin-lattice relaxation time  $T_1$  of the slowest relaxing HC in the used NG mixture [45]. Moreover, it is much larger than the  $T_1$  relaxation time of 0.53 s of the binary  $\text{H}_2\text{O}$ -TEG mixture with 22.5 wt% water content used in this work as determined by the inversion-recovery method.

The proton spectra were recorded following the strategy recently proposed in Ref. [49]. This included single-scan acquisition, magnetic field shims based on the methane peak after 20 scans to maintain the spectra quality, and spectra alignment using the signal of methane set at 0 ppm. For each recorded spectrum, the time domain signal was zero filled to 256 k points before the Fourier transformation. Baseline and phase correction of the spectra were not necessary. Due to the increased spectral distortions detected on the recorded spectra of the NG sample under the presence of the contaminants, additional quality control (QC) parameters to those introduced in Ref. [49] were developed and introduced in this work.

For quantifying the LOD and LOQ of TEG with the used HP tube, in the first step a determination of the position and the length of the sensitive volume was done using a water sample and a high-precision pipette. In the second step, the maximum amount of TEG inside the sensitive volume was determined using the determined length of the sensitive volume, the known value of the inner diameter of the HP tube, and by using a density of 1.1  $\text{g}\cdot\text{ml}^{-1}$  [50]. The obtained value of 57 mg was in excellent agreement with the value determined via the volume of the water in the sensitive volume (detailed information of this procedure is given in SI).

For the generation of samples with different amounts of TEG in the sensitive volume in the presence of NG, spacers with a thickness of 0.5 mm were added one by one under the PEEK cap. The quantification of different TEG amounts was done using two methods: 1) by knowing the thickness of the spacer, the inner diameter of the HP tube, and the above mentioned density of TEG, and 2) by NMR itself by simple signal integration and by considering the linear proportionality with the integral of the maximum amount of TEG in the sensitive volume.

#### 2.5. Indirect hard modelling methodology

Indirect hard model (IHM) is based on a physically motivated concept to perform quantitative analysis on a mixture spectrum. Although IHM was originally introduced for the spectral analysis in Raman and mid-IR spectroscopy [51], its suitability was demonstrated also for NMR spectroscopy [52–55]. An IHM is composed of individual

hard models (HMs) which are parameterized peaks of pure components spectra. Each HM is defined by the superposition of Pseudo-Voigt peaks which are a linear combination of a Lorentzian and a Gaussian function. When these HMs are fitted into an unknown spectrum, the Pseudo-Voigt functions are adjusted in terms of peak width, intensity, and position. All these parameters are adjusted in an iterate way such that the root-mean-square (RMS) between the new spectrum and the fit model is minimized. This flexible approach allows IHM to account for both linear and non-linear spectral variations, thereby having the potential to drastically reduce calibration efforts when compared with traditional chemometric methods, e.g., Partial Least Squares (PLS) where large amounts of data are required to train the models.

The individual hard models developed for methane (C1), ethane (C2), and propane (C3) were taken from our previous work [49]. The IHM fit parameters were set as follows: maximal interactions for the fitting mode, 0.02 ppm of tolerance in the chemical shift variation for the whole model and for the individual peaks. During the initial fitting of the IHM to the recorded spectra, the C1 model was used not only for dry gas as implemented in our previous work but also for the wet gas, where the C1 signal undergoes strong distortions due to the presence of various amounts of liquid TEG. Including the C1 model ensured that the hard models of C2 and C3 remained confined to their respective domains, preventing them from erroneously fitting the deformed left flank of the C1 signal. Subsequently, as presented in our previous work [49], after fitting the IHM, the hard model of C1 was manually deleted, since even small mismatches in the integral of this species led to large errors in the composition analysis. Its final integral was then determined by calculating the difference between the summed areas of the fitted hard models of the C2 and C3 components and the area of the entire spectrum. The IHM analysis was carried out with the PEAXACT software package (S-PACT GmbH, Aachen, Germany) version 5.5.

### 3. Results and Discussions

#### 3.1. $^1\text{H}$ Nuclear Magnetic Resonance spectrum of natural gas in presence of triethylene glycol as a liquid contaminant

Typical proton low-field NMR spectra of gaseous NG in the presence of the aqueous TEG are depicted in Fig. 2. The TEG sample has two signals: one due to the methylene group ( $\text{CH}_2$ ) and one of the hydroxyl (OH) group with the water signal on top of it, in agreement with literature [56,57]. The  $^1\text{H}$  spectrum of the gas mixture is more complex but with signals far away from the signals of TEG. The methane signal is well separated from the other signals while the ethane and propane peaks exhibit an overlapping which impedes in this case their quantitative composition analysis by simple signal integration. Thus, more advanced analytical methods such as IHM can be applied [45,58]. The good differentiation between the signals of the TEG and NG already highlights the possibility to quantify both components inside the gas-liquid mixture.

In view of the scope of the current work it is also important to gain a deeper understanding of the effect of TEG on the spectra quality. Therefore, proton spectra were acquired for NG pressurized at 200 bars and at various TEG amounts up to 57 mg. The latest amount corresponds to the amount needed to fully occupy the sensitive volume. For this, TEG was placed at the bottom of the tube and then the NG sample was added. For simulating samples with different amounts for TEG inside the sensitive volume, as explained in the experimental section, the NMR tube was raised step-by-step inside the NMR spectrometer with the help of spacers. In addition, with this approach an improved understanding of the effect of stationary TEG at different positions inside the sensitive volume on the spectra quality should be gained. The obtained results are depicted in Fig. 2. The maximum determined error of these data was of 1.15 %. Please note that Fig. 2b include only the recorded data in the linear regime. Non-linear effects were observed at low TEG amounts which correspond to the region where the radiofrequency coil starts.

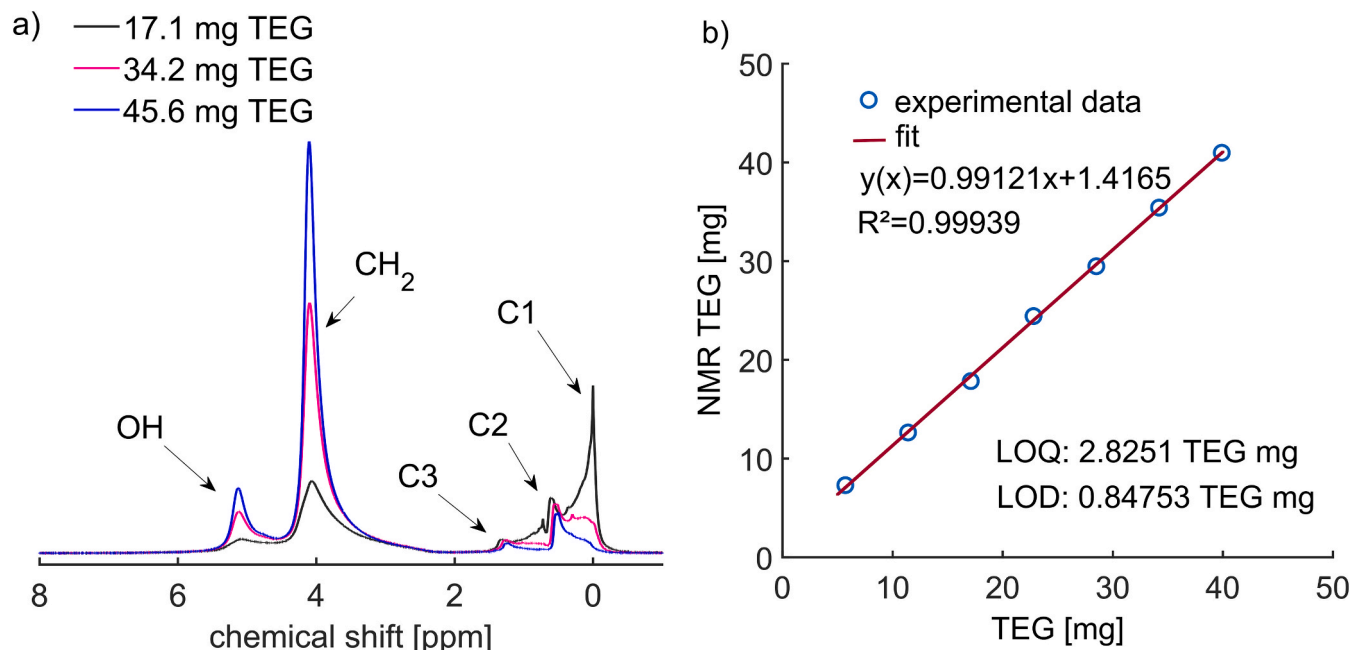


**Fig. 2.** (a) Exemplarily  $^1\text{H}$  NMR spectra of NG containing methane (85 mol%), ethane (10 mol%), and propane (5 mol%) recorded at 200 bar in the presence of various amounts of TEG and using 1 scan, which translates in 2 min measuring time. (b) Determined LOD and LOQ for TEG in the sensitive volume were obtained from the TEG-NG sample pressurized at 200 bar, using spectra recorded with a single-scan.

As expected, the amount of the gas sample available in the sensitive volume is reduced with increasing the TEG content. This is accompanied by an increase in the linewidth of the gas signals leading to a loss in the spectral resolution owed to the increased signal overlapping between the methane peak and the peaks of the two other HCs. To get a better overview of the changes induced by the presence of TEG, the linewidth of the methane peak at 50 % heights was tracked. In our previous work, it was shown that this linewidth can be used as a quality control parameter to monitor the quality of the recorded spectra [49,59]. In addition to this linewidth, the linewidth at 10 % signal height was also quantified here. Determined values are reported in Table 1. The quantification of the C1 linewidth at 50 % could be done only up to a TEG amount of about 28.5 mg. This is because beyond these values, the  $\text{CH}_2$  peak of TEG became predominant in the recorded spectra and the automatic shim uses this signal for the optimization of the magnetic field homogeneity with the consequence that the TEG signals are improved but not those from NG. No attempt was done to use a manual shim procedure to improve the NG signals as well, as this will not be a feasible option for in-field applications. As depicted in Fig. S12, a linear correlation was observed between the mentioned TEG amount and the C1 linewidth at 50 % height. The identification of the type of correlation is important for defining threshold values of the QC parameter based on this linewidth (see section about the QC) also for TEG concentrations not directly measured within this work. Regarding the linewidth at 10 %, it

**Table 1**

Dependence of the linewidth at 50 % and respectively 10 % signal height in the C1, C2, and C3 gaseous mixture measured at 200 bar in the presence of various TEG amounts in the sensitive volume.

TEG [mg]	linewidth at 50 % C1 signal height [Hz]	linewidth at 10 % C1 signal height [Hz]
34.2	—	—
28.5	7.47	—
22.8	5.95	—
17.1	4.34	—
11.4	3.35	31.89
5.7	2.21	21.21
0	1.35	14.19

could be directly determined from the spectrum only up to 11.4 mg TEG content due to the increased signal distortion and overlapping HC peaks.

In the next step, the LOD and LOQ of TEG in the HP-tube in presence of the NG sample at 200 bar was determined. According to the approach used in Ref. [60],  $\text{LOQ} = 10 \cdot \sigma / S$  and  $\text{LOD} = 3.3 \cdot \sigma / S$ , where  $\sigma$  is the standard deviation of the response and  $S$  the slope of a calibration curve of known analyte concentrations (please see SI for more details). For this purpose, the correlation between the mass values predicted with NMR and the known TEG amounts in the sensitive volume, determined by the upward displacement of the sapphire tube within the sensitive volume by adding the spacers with well-defined thickness, was analyzed (Fig. 2b). Under the used experimental conditions, 0.85 mg TEG can be reliably identified and 2.83 mg respectively quantified.

### 3.2. Quality control parameters for $^1\text{H}$ Nuclear Magnetic Resonance spectra of natural gas in presence of liquid contaminants

High quality data is necessary to ensure excellent results in analytical methods. In the realm of NMR, diverse strategies are used to cope with experimental variations and to ensure the reproducibility of high-quality spectra [49,61]. For instance, NMR spectroscopists periodically optimize the magnetic field homogeneity to maintain the linewidth of spectra during the measurement [49,61,62]. Subsequently, the recorded spectra goes through a peak shape quality assessment in order to ensure key spectral features within predefined thresholds [49,61]. Further corrections in the baseline and phase have to be considered since even small deviations affect the quality of the derivate quantitative analysis [61,62]. Good and reproducible signal quality are main requirements to guarantee the reliability of various data analysis methods [49,53].

While modern high-field NMR devices are capable of maintaining a high level of magnetic field stability over extended periods of time [61], the design of the benchtop NMR spectrometers is based on rare earth permanent magnets. These magnets are sensitive to external temperature variations that lead to magnetic field instabilities [63]. To perform the quantitative analysis of pressurized natural gas samples up to 200 bar while accounting for this magnetic field instabilities, a refined experimental methodology, which consisted in single-scan acquisition and two quality control parameters to select the adequate spectra for

further analysis, was proposed in our previous work [49]. The QCs were the linewidth at 50 % height (full width at half height, FWHM) of the methane peak and the integral over all signals as primary indicators of the signal width stability and sample detection leakage respectively [49]. In addition, this higher quality spectrum is more suitable for the IHM analysis. Yet, in presence of aqueous TEG in the natural gas, additional spectra indicators are identified and included as quality control parameters due to the increased complexity of signal distortions detected in the  $^1\text{H}$  NMR spectra.

In the first step, the linewidth at 10 % methane peak height was established as it provides additional information regarding peak base deformation. In addition, peak shape symmetry-related indicators are defined using the linewidths of methane signal at 10 % and 50 % peak height. For this reason, the parameters  $a_1$ ,  $a_2$ ,  $b_1$ , and  $b_2$  are defined (Fig. 3a). Here,  $a_1$  and  $a_2$  correspond to the horizontal distance between the vertical projection of the maximum peak height to the left- and to the right-flank at 50 % peak height of the methane signal respectively. Analogous definition applies to  $b_1$  and  $b_2$  but at 10 % peak height of the methane signal. Considering these new parameters, we introduced the peak symmetry at 10 % ( $\Delta_{10\%}$ ) and 50 % ( $\Delta_{50\%}$ ) peak height as defined by Eqs. (1) and (2) respectively. The new QC indicators are 1 in the ideal case. Yet, in the case of our study, their values are lower than 1, i.e. indicating asymmetrical peaks. As previously explained [45,47,49], the ideal peak shapes couldn't be achieved due to remaining surface inhomogeneities after the manufacturing process of the HP-tube and the inherent magnetic field inhomogeneity of the benchtop NMR equipment. A third QC parameter,  $\Delta_{\text{signal}}$ , was introduced to characterize the symmetry of the whole signal as a ratio of the slopes of both the left- and right-flank of the methane signal. This  $\Delta_{\text{signal}}$  parameter, presented in Eq. (3), considers the ratio of the horizontal differences  $b_2 - a_2$  and  $b_1 - a_1$  for the left and the right side of the methane signal, respectively. For the calculations, the magnitude values of both differences are considered. A peak with good symmetry would have a slope ratio close to 1. Nevertheless, one needs to mention that the slope ratio can be close to 1 even if the highest portion above the 50 % peak height is experiencing deformations. These new introduced QC parameters add thus more peak shape criteria because they can respond to the displacement of the position of the signal maximum and shoulders formation while the two linewidths may remain unaltered during this signal distortion process.

$$\Delta_{10\%} = b_1/b_2 \text{ if this ratio exceeds 1, else } \Delta_{10\%} = b_2/b_1 \quad (1)$$

$$\Delta_{50\%} = a_1/a_2 \text{ if this ratio exceeds 1, else } \Delta_{50\%} = a_2/a_1 \quad (2)$$

$$\Delta_{\text{signal}} = (b_2 - a_2)/(b_1 - a_1) \text{ if this ratio exceeds 1, else } \Delta_{\text{signal}} = (b_1 - a_1)/(b_2 - a_2) \quad (3)$$

The above introduced QC parameters allow to identify the best reproducible single-scan spectra. Fig. 3b illustrates the complete set of QC parameters implemented to 140 single-scan spectra of the three-component gaseous mixture considered in this study. Pronounced variations in the QC values are observed in the first 40 recorded spectra (region labeled as A in Fig. 3b). During this initial period, while the linewidths remain largely constant, the symmetry QC parameters exhibit fluctuations. These changes can be attributed to a combination of factors, including a thermal stabilization period following the insertion of the NMR tube into the spectrometer and room temperature variations [45,46,49]. Consistent with our previous work [49], magnetic field homogeneity was preserved with the inclusion of shim protocols each 20 measurements [49,59]. This is reflected in steady and reproducible linewidth values as measuring time increases. As shown in Fig. 3b, region B, after the first 40 scans immediately following each magnetic field shim, the QC parameter values are constant during the remaining spectral acquisition. During the measurement period, no appreciable variations in linewidth or in symmetry QCs of the methane signal were observed. Under the experimental conditions in the region marked with B in Fig. 3b, the room temperature reached a steady state and the signal quality remains largely constant [47,59].

Following the same approach as in our previous work [49], the thresholds of the quality parameters without TEG in the sensitive volume for the pure natural gas sample containing C1, C2, and C3 were defined by selecting previously recorded spectra of homogeneous and reproducible peak shapes based on visual inspection. Their consolidated values with their standard deviation were:  $0.99 \pm 0.06$  Hz and  $2.30 \pm 0.06$  for the linewidth at 50 % and at 10 % respectively. The values of the symmetry parameters were:  $\Delta_{50\%} = 0.51 \pm 0.06$ ,  $\Delta_{10\%} = 0.72 \pm 0.06$ , and  $\Delta_{\text{signal}} = 0.91 \pm 0.06$ . Table S12 lists the values of the parameters obtained for the same natural gas sample with various TEG amounts in the sensitive volume. These values were included in the MATLAB script with a tolerance of 10 % regarding each averaged value for an automatic selection of the single-scan spectra that meet these QC criteria. Under the used experimental conditions in this work, the new QC parameters could be used to assess the symmetry and signal quality up to 11.4 mg TEG since up to this amount the linewidth at 10 % peak height could be determined. For 28.5 mg TEG amount in the sensitive volume, the QC parameters used in our previous work [49] could be implemented since the FWHM could be determined up to this value as indicated in Table 1. For this, its threshold values were set according to the values listed in

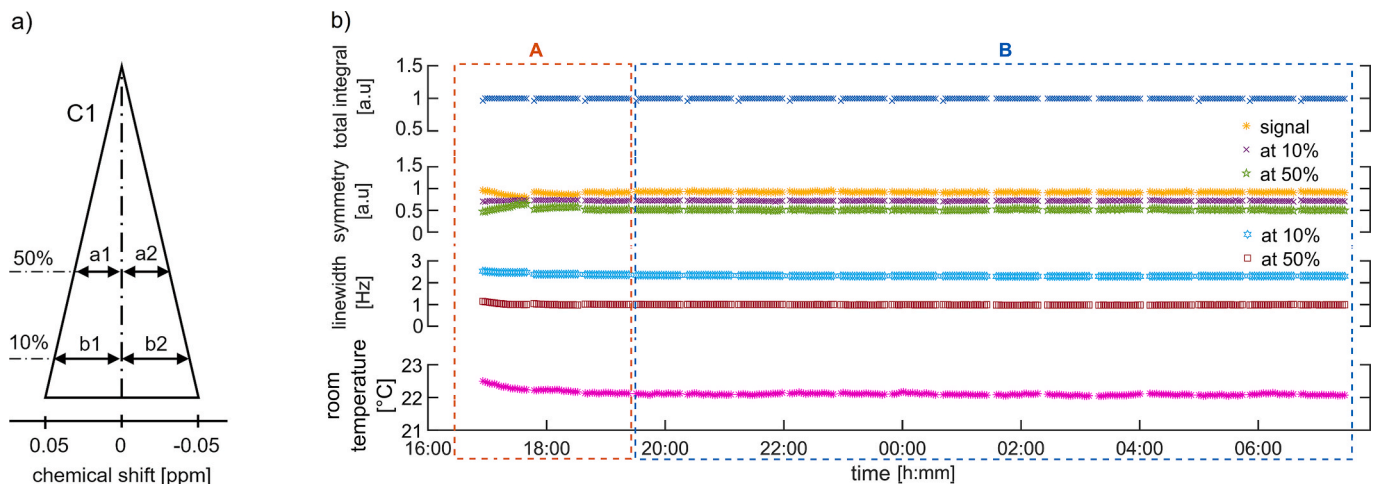


Fig. 3. QC parameters: a) graphical description using the C1 signal. The meaning of  $a_{1,2}$  and  $b_{1,2}$  are given in the text. b) values of the QC parameters for 140 single-scan  $^1\text{H}$  NMR spectra of three components gaseous mixture along with the variation of the room temperature extracted from the spectrometer's log file.

**Table 1.** This less rigorous spectra selection lead to a higher error in the quantitative analysis but still maintaining a good agreement with the values of references as explained in the [section 3.3](#) of this manuscript. At higher amounts of TEG in sensitive volume, the reduced amount of the gas samples in the sensitive volume and the poor resolution of the recorded spectra hampered the proper species recognition with the IHM.

### 3.3. Natural gas composition analysis in the presence of stationary triethylene glycol in the sensitive volume

The performance of the IHM was tested for the composition analysis of the  $^1\text{H}$  NMR spectra recorded at 200 bar of the selected natural gas sample with various amounts of TEG in the sensitive volume under stationary conditions by using large sets of single-scan spectra: 1) at 0 mg TEG, with TEG being located at the bottom of the HP tube, right below the sensitive volume; 2) at 5.7 mg TEG where the amount of aqueous TEG is higher as the determined LOQ; 3) at 11.4 mg TEG in the presence of the highest possible amount of aqueous TEG at which the QC parameters developed in this work could still be implemented and 4) at 28.5 mg TEG owed that until this amount in the sensitive volume was possible to use the parameters introduced in our previous work [49] since the measurement of the FWHM was still possible. Fig. 4a depicts a

$^1\text{H}$  NMR mean spectrum consisting of 64 single-scan spectra of the TEG-NG matrix sample with 11.4 mg of aqueous TEG sample in the sensitive volume. The averaged selected spectra were appropriated to ensure a sufficient signal to noise ratio for the small signals from C3. Here, it is shown that despite of the similar signal intensity contribution of the TEG sample to the  $^1\text{H}$  NMR spectra in comparison to the NG signal intensity, IHM could properly fit the various components contributing to the  $^1\text{H}$  NMR signals of the gas sample.

The determined molar concentrations of the species C1, C2 and C3 present in the NG sample using IHM at different aqueous TEG amounts are presented in Fig. 4b. Similar to our previous work [45,49], the comparison between the NMR results and the values of reference is done by using the degree of equivalence method proposed in Ref. [64]. For the pure gas sample, the recorded spectra were highly reproducible with minor peak shape deviations between the recorded single-scan spectra. This can explain the low dispersion of the results obtained with IHM as presented in Fig. 4b and the excellent agreement with the vendor certificate. At TEG amounts of 5.7 mg and 11.4 mg, a larger measuring time was necessary until enough single-scan spectra that met the QC criteria were accumulated to obtain the three 64 scans multi-scan spectra. For these two cases, the predicted results with IHM led to a similar grade of uncertainties (Fig. 4b). For the  $^1\text{H}$  NMR spectra of the gas sample in

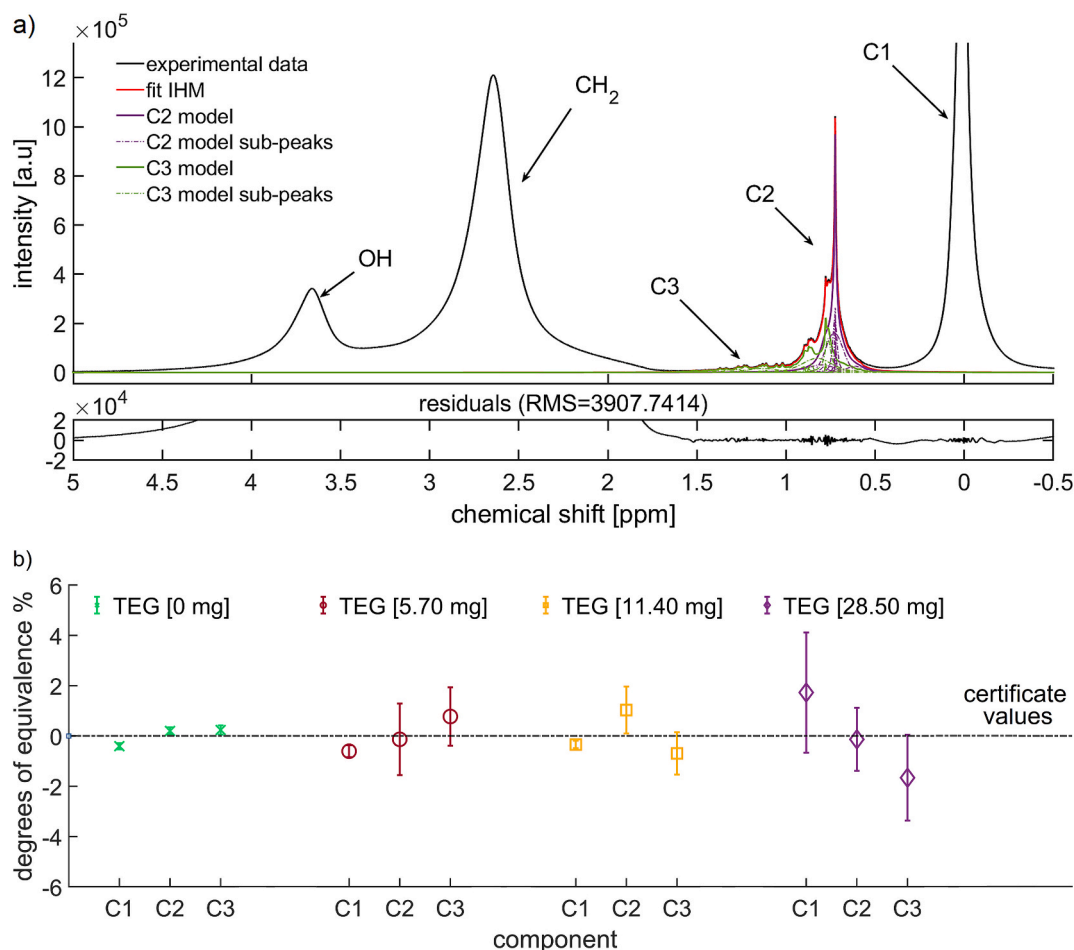


**Fig. 4.** (a) Exemplarily indirect hard model fit on a spectrum of a ternary gaseous mixture in presence of 11.4 mg of aqueous triethylene glycol. As the IHM was conducted only on the signals of the NG, the residual value is low only on this region. As explained in [section 2.5](#), after fitting the whole components of the IHM, the C1 integral was obtained by subtracting from the total gas integral the integral of the frequency domain in the range 0.5 and 1.8 ppm corresponding to the areas of C2 and C3 components. (b) Comparison of IHM quantitative composition analysis results with the reference values by using the degrees of equivalence for the ternary gaseous mixture containing various aqueous TEG contents in the NMR sensitive volume. Here the degrees of equivalence are used in the same way as in Refs. [49,58], where the disparity between the predicted NMR results and the certificate values are shown. For each experiment, at the specified TEG amount in the sensitive volume, three multi-scan spectra consisting of 64 scans were analyzed. The error bars represent the standard deviations of the average differences between the determined composition and the certificate values.

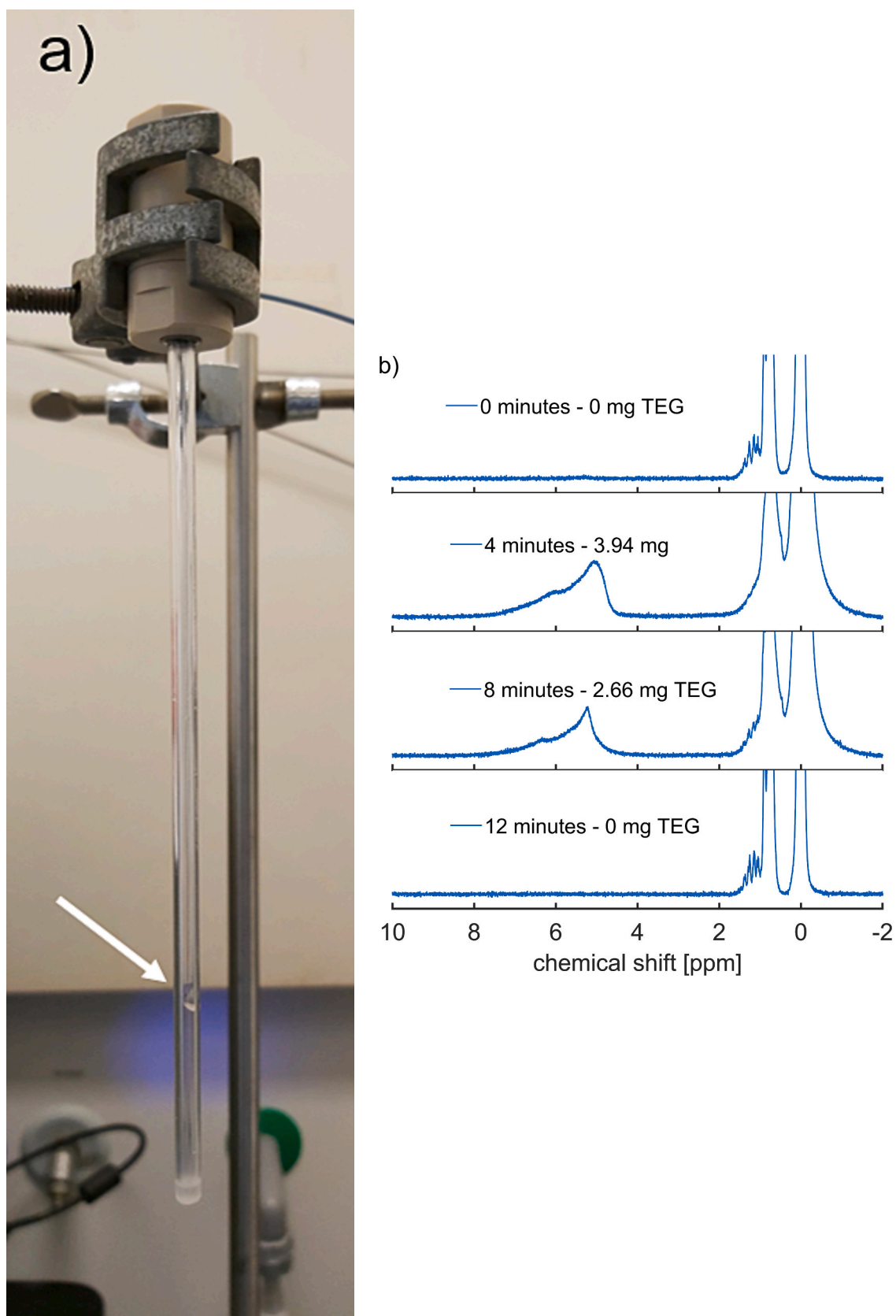


**Fig. 5.** Droplet experiment: a) Aqueous TEG droplet moving inside the HP-tube from top to bottom. Selected online single-scan  $^1\text{H}$  NMR spectra of the TEG-gas with the TEG droplet moving through the sensitive volume: b) Proton NMR spectra showing the signals of TEG and the gas sample. The spectra are zoomed for better view of the TEG signals. c) Spectral region corresponding to the signals of the gas sample for better observation of the changes in the spectra quality.

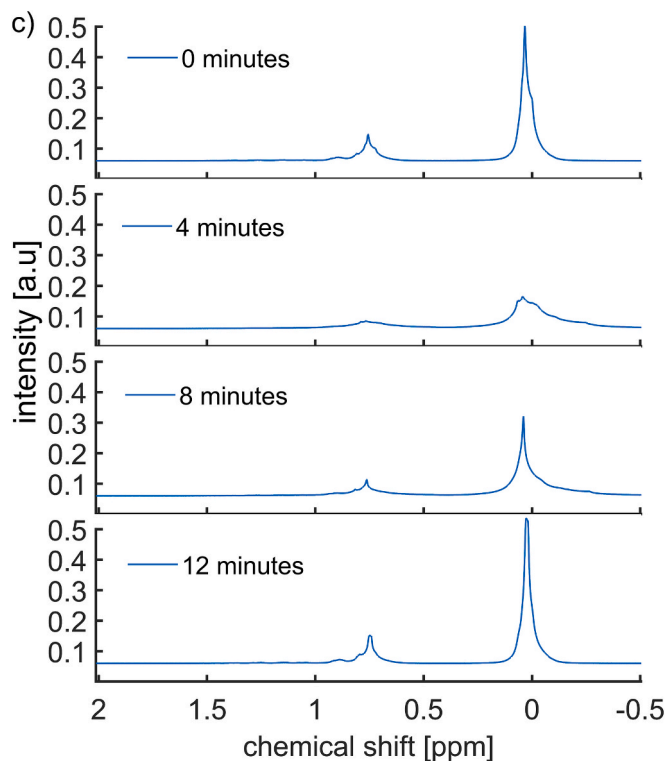


Fig. 5. (continued).

presence of a TEG amount of 28.5 mg, the spectra were selected considering only the linewidth at 50 % methane peak height which significantly reduced the peak shape constraints during the spectra selection. Therefore, the predicted results show larger dispersion and larger difference to the vendor certificate.

In the context of official regulations, the QC parameters developed in this work enabled the determination of molar concentrations with uncertainties below 0.1 mol% for the three NG components using NMR. These uncertainties are within the accepted limits of up to 0.15 mol% for smaller HCs according to ASTM D 1945 serving as the primary reference. In presence of 5.4 mg and 11.4 mg TEG, even though the average values were higher than the references, they were obtained with a similar dispersion regarding the vendor certificate. Thus, we strongly believe that in on-line applications requiring the composition analysis of natural gas after dehydration process, the QC parameters introduced in this work will enhance the robustness of HP-NMR spectroscopy.

### 3.4. Effects of liquid droplets on the $^1\text{H}$ Nuclear Magnetic Resonance spectra of the natural gas sample

After leaving the glycolic dehydration unit, traces of TEG could be present in form of droplets in the dried natural gas stream [9]. To investigate the droplet effect on the recorded  $^1\text{H}$  NMR spectra quality of the selected NG sample, single-scan spectra were recorded while the TEG droplet was moving through the HP-tube (Fig. 5a). Here only the spectra recorded during the timeframe on which the droplet passes the NMR sensitive volume are presented with the time 0 been defined as the time before the droplet enters the sensitive volume (Fig. 5 and Fig. SI3). Fig. SI3 shows the changes in the integral of the gas sample starting from the defined time zero. As expected, it decreases in the presence of the TEG droplet, which causes a displacement of the gas sample outside the sensitive volume over time. From these data it was estimated that the droplet moves with an average speed of 0.5 mm/min through the sensitive volume. The passing of the TEG droplet through the sensitive volume can be observed in Fig. 5b which depicts the portion of the proton spectrum corresponding to the aqueous TEG droplet being

detected at different moments. During the minute 4, the droplet could be detected as being most of it inside the sensitive volume with its  $^1\text{H}$  NMR signal overpassing the LOQ. After 8 min, only a part of the droplet can still be detected while after 12 min the droplet exited the sensitive volume. Since the  $T_1$  relaxation time of the TEG sample is dramatically shorter than that of the gas sample, a repetition time of about 3 s would be enough to acquire quantitative TEG  $^1\text{H}$  NMR spectra at a higher temporal resolution under the experimental conditions presented here. No attempt was made during this study to conduct such measurements.

The effect of the liquid droplet on the  $^1\text{H}$  NMR spectra of the natural gas is depicted in Fig. 5c. At the minute 0 right before the droplet entered in the sensitive volume, an initial spectral resolution degradation could be observed by simple visual inspection. Between the minute 4 and 8, when most of the droplet was present in the sensitive volume, the distortions were even more dramatic. After minute 12, when no residual signal of the droplet could be detected anymore, the implementation of a shim protocol was necessary to fully recover the quality of the  $^1\text{H}$  NMR spectra of the gas sample. Although the dynamic droplet strongly affected the quality of the  $^1\text{H}$  NMR spectra of the gas sample, the developed QC parameters could be implemented to identify the full recovery of the spectra quality after the shim protocol routine and proceed with further analysis. For instance, once the droplet exited the sensitive volume and after the first magnetic field shim, a multi-scan spectrum containing 64 single-scan spectra could be obtained with the new QC parameters and analyzed using IHM. The analysis yielded compositions of 85.61 mol%, 9.60 mol% and 4.79 mol% for C1, C2 and C3 respectively. The obtained results are highly consistent with the vendor certificate proving the effectiveness of the new QC parameters in selecting spectra of optimal quality while simultaneously allows to discard the spectra affected by unpredictable contaminant droplets.

### 3.5. Our current vision to implement the NMR method for in-field measurements

The measurements presented in the previous sections were conducted in a transparent high-pressure tube to aid in visualizing the

position of the TEG inside it. This contributes to a better understanding of the effect that the presence of TEG has on the experimental results. Yet, the presence of a single tube opening will lead over time to the accumulation of amounts of TEG which will not hinder the NMR detection of the gas signal as long as gas is present in the sensitive volume but its composition analysis. Thus, the accumulated TEG has to be removed. While this is an easy task in laboratory, it poses additional challenges for in-field measurements as it requires the removal and cleaning of an expensive and easy to damage NMR tube. In addition, we also observed that the passing of a droplet inside the sensitive volume leads to strong signal deformation of the gaseous phase, hindering the composition analysis during this passing time. Thus, for the implementation of the NMR method under a real in-field scenario, we envisage that the measurements will be conducted under a stop-flow manner by using a flow-through tube with two openings placed inside the NMR spectrometer. The sample to be measured will be dispatched inside the tube having the bottom opening closed and then the top opening will be also closed. Given that one can conduct single-scan measurements and by using the implemented QCs, the moment at which a droplet passes the sensitive volume can be identified. Given that the required length of a flow-cell for NMR Spinsolve is about 50 cm, most probably most of the accumulated TEG will be at its bottom and thus being outside the sensitive volume will not be observed. Then, a quick shim can be conducted and the acquisition of the proton spectra of the stationary sample inside the sensitive volume can be done. In addition, the full set of QCs introduced in this work can be implemented to ensure the quality of the recorded spectra for the gas sample. Even though TEG may still be present, as long as its amount does not exceed the maximum reported value for this type of high-pressure tube, the composition analysis of the NG samples remains possible. Once the number of necessary scans are acquired, the flow-cell will be opened at the bottom part to release the sample inside. In such way, an accumulation of the liquid sample at the bottom of the tube to hinder the analysis will be avoided. In this case, no further step for removal of the contamination will be needed. In addition, the foreseen flow tube is built using a plug-in method and it is low cost such that, if needed, it can be easily exchanged from time to time. The key advantage of our method is that even if TEG may remain as a film on the NMR tube walls, this does not pose an impediment on the composition analysis of the NG samples as observed for other advanced analytical methods.

While in the here reported study, only a ternary gaseous sample was considered as a proof-of-concept, the successful application of the HP NMR spectroscopy in combination with IHM for dry gaseous mixtures containing near methane, ethane, and propane also n-butane, *iso*-butane, n-pentane, *iso*-pentane, neo-pentane, and n-hexane has been previously demonstrated [45,49]. Therefore, we expect that the proposed strategy will work under field conditions also for gaseous components containing such higher order HCs.

#### 4. Conclusion

The application of HP low-field proton NMR spectroscopy for the composition analysis of recorded spectra of natural gas in presence of liquid contaminants was demonstrated for the first time. The methodology was shown on an exemplarily NG gas sample containing methane, ethane, and propane in the presence of aqueous TEG as a representing liquid contaminant under static and dynamic conditions.

In addition, the experimental approach introduced in our previous work was boosted with four new QC parameters based on the methane signal to improve signal characterization: linewidth at 10 %, peak symmetry at 50 % and 10 % peak height, and signal symmetry from the slopes of the methane peak's flanks. These QC criteria were applied on recorded  $^1\text{H}$  NMR spectra of the NG sample pressurized at 200 bar in the presence of TEG in the sensitive volume.

For the stationary condition, high-quality  $^1\text{H}$  NMR single-scan spectra were selected using the QC parameters, resulting in multi-scan

spectra that yielded reproducible results and composition in excellent agreement with the vendor certificate, up to a TEG amount of 28.5 mg in the sensitive volume. Under dynamic conditions, despite strong spectral distortions from a flowing droplet, the QC parameters effectively identified high-quality spectra after magnetic field shimming.

Furthermore, it was demonstrated that the used  $^1\text{H}$  NMR spectroscopy method can quantify not only the gas composition but also the amount of TEG present along with the gas phase inside the sensitive volume under stationary conditions. In the case of moving TEG droplets, reliable quantification depends on how long the entire droplet remains within the coil during the measurements. Due to the long repetition time required for the  $^1\text{H}$  NMR signal acquisition of the natural gas sample, the droplet would have to reach a stationary condition or move such slow that it is the whole time within the sensitive volume during data acquisition. Such a condition is unlikely during in-line applications given that the velocity of natural gas in the pipeline is at least on the order of  $\text{m}\cdot\text{s}^{-1}$ . Therefore, although spectral distortions caused by dynamic droplets on the  $^1\text{H}$  NMR signal of the gas sample can be detected, quantification of TEG droplets is not possible with the present method. The LOD, LOQ, and maximum possible TEG amounts were determined to be 0.85 mg, 2.83 mg, and 57 mg, respectively.

In conclusion, this work demonstrates the robustness of HP-NMR spectroscopy for the composition analysis of wet gas mixtures in in-field applications, where liquid contaminants could compromise the quantitative performance of traditional analytical methods.

#### CRedit authorship contribution statement

**S.A. Ortiz Restrepo:** Writing – original draft, Methodology, Investigation, Formal analysis, Data curation, Conceptualization. **J. Denninger:** Writing – review & editing, Methodology, Investigation. **P.M. Dupuy:** Writing – review & editing, Validation, Resources, Methodology. **H.C. Widerøe:** Writing – review & editing, Validation, Resources, Methodology. **O. Mohnke:** Software, Resources, Methodology, Data curation. **Ø. Leknes:** Visualization, Resources. **A. Adams:** Writing – review & editing, Supervision, Project administration, Methodology, Funding acquisition, Conceptualization.

#### Declaration of competing interest

The authors declare that they have no known competing financial interests or personal relationships that could have appeared to influence the work reported in this paper.

#### Acknowledgments

We acknowledge the financial support from Equinor, Gassco, and Baker Hughes. We also thank Dr. Jürgen Kolz from Magritek for his support with the Spinsolve hardware and software. We are also grateful to the editor and the referees for their valuable comments and suggestions to improve the quality of our manuscript.

#### Appendix A. Supplementary data

Supplementary data to this article can be found online at <https://doi.org/10.1016/j.enconman.2025.120258>.

#### Data availability

Data will be made available on request.

#### References

- [1] IEA. Global Energy Review 2025. 2025.
- [2] IEA. Gas Market Report, Q1-2025. 2025.
- [3] Iea. World Energy Balances Database documentation April 2025 edition. IEA Family and Beyond; 2025.

- [4] Al-Yafei H, Aseel S, Kucukvar M, Onat NC, Al-Sulaiti A, Al-Hajri A. A systematic review for sustainability of global liquified natural gas industry: a 10-year update. *Energy Strat Rev* 2021;38:100768. <https://doi.org/10.1016/j.esr.2021.100768>.
- [5] Bistline JET, Young DT. The role of natural gas in reaching net-zero emissions in the electric sector. *Nat Commun* 2022;13:1–11. <https://doi.org/10.1038/s41467-022-32468-w>.
- [6] Cozzi L, Gould T, Bouckart S, Crow D, Kim T-Y, McGlade C, et al. World energy outlook 2020. IEA 2020;2050:213–50. [https://doi.org/https://www.oecd-ilibrary.org/energy/world-energy-outlook-2020\\_557a761b-en](https://doi.org/https://www.oecd-ilibrary.org/energy/world-energy-outlook-2020_557a761b-en).
- [7] Palma A, Paltrinieri A, Goodell JW, Oriani ME. The black box of natural gas market: past, present, and future. *Int Rev Financ Anal* 2024;94. <https://doi.org/10.1016/j.irfa.2024.103260>.
- [8] Yarlagaadda B, Iyer G, Binsted M, Patel P, Wise M, McLeod J. The future evolution of global natural gas trade. *IScience* 2024;27. <https://doi.org/10.1016/j.isci.2024.108902>.
- [9] Wang X, Economides M. Natural Gas Processing. In: *Advanced Natural Gas Engineering*. Gulf Professional Publishing, pp. 115–169. *Advanced Natural Gas Engineering* 2009:115–69. <https://doi.org/10.1016/b978-1-933762-38-8.50011-3>.
- [10] Soroodan E, El-Okazy MA, Macario E, Kentish SE. Triethylene Glycol Solubility in High-pressure methane: New Experimental Data at 40 to 60 °C. *Ind Eng Chem Res* 2024;63:2895–900. <https://doi.org/10.1021/acs.iecr.3c04002>.
- [11] Zhao J, Wang Z, Zhao S, Ye H, Shen K. Study on the mechanism of decomposition of methane hydrate by the compound inhibitor. *Sci Rep* 2025;15:5896. <https://doi.org/10.1038/s41598-025-90241-7>.
- [12] Bahraminia S, Ambia M, Koohsaryan E. Dehydration of natural gas and biogas streams using solid desiccants: a review. *Front Chem Sci Eng* 2021;15:1050–74. <https://doi.org/10.1007/s11705-020-2025-7>.
- [13] Kong ZY, Mahmoud A, Liu S, Sunarso J. Revamping existing glycol technologies in natural gas dehydration to improve the purity and absorption efficiency: Available methods and recent developments. vol. 56. Elsevier B.V.; 2018. <https://doi.org/10.1016/j.jngse.2018.06.008>.
- [14] Petropoulou EG, Carollo C, Pappa GD, Caputo G, Voutsas EC. Sensitivity analysis and process optimization of a natural gas dehydration unit using triethylene glycol. *J Nat Gas Sci Eng* 2019;71:102982. <https://doi.org/10.1016/j.jngse.2019.102982>.
- [15] Liang H, Huang Q, Li X, Wu Q, Yan H, Meng J, et al. Investigation of the Factors and Mechanisms Affecting the Foaming of Triethylene Glycol in Natural Gas Purification. *Processes* 2025;13:1261. <https://doi.org/10.3390/pr13051261>.
- [16] Rahmaman N, Söyler N, Wande FM, Hashemi H. An investigation on hydrate prediction and inhibition: an industrial case study. *Can J Chem Eng* 2024. <https://doi.org/10.1002/cjce.25357>.
- [17] Santos CIAV, Barros MCF, Ribeiro ACF, Bou-Ali MM, Mialdun A, Shevtsova V. Transport properties of n -ethylene glycol aqueous solutions with focus on triethylene glycol-water. *J Chem Phys* 2022;156. <https://doi.org/10.1063/5.0091902>.
- [18] Shoukat U, Baumeister E, Knuutila HK. ATR-FTIR model development and verification for qualitative and quantitative analysis in MDEA–H<sub>2</sub>O–MEG/TEG–CO<sub>2</sub> blends. *Energies (Basel)* 2019;12. <https://doi.org/10.3390/en12173285>.
- [19] Shilliday ER, Barrow B, Langford D, Ling NNA, Robinson N, Johns ML. Quantitative measurement of Mono-Ethylene Glycol (MEG) content using low-field Nuclear magnetic Resonance (NMR). *J Nat Gas Sci Eng* 2022;101:104520. <https://doi.org/10.1016/j.jngse.2022.104520>.
- [20] Standards Norway. NORSOK P-002:2023 AC:2024. Process Design. Lysaker, Norway: Standards Norway 2024.
- [21] International Organization for Standardization. ISO 10715:2022. Natural gas — Gas sampling. Geneva, Switzerland: ISO 2022.
- [22] ISO International organization for standardization. In: *natural gas - determination of composition and associated uncertainty by gas. chromatography* 2012:05.
- [23] Brown AS, Milton MJT, Cowper CJ, Squire GD, Bremser W, Branch RW. Analysis of natural gas by gas chromatography: Reduction of correlated uncertainties by normalisation. *J Chromatogr A* 2004;1040:215–25. <https://doi.org/10.1016/j.chroma.2004.04.007>.
- [24] Rhoderick GC. Analysis of natural gas: the necessity of multiple standards for calibration. *J Chromatogr A* 2003;1017:131–9. <https://doi.org/10.1016/j.chroma.2003.08.002>.
- [25] Karpash O, Darvay I, Karpash M. New approach to natural gas quality determination. *J Pet Sci Eng* 2010;71:133–7. <https://doi.org/10.1016/j.petrol.2009.12.012>.
- [26] International Organization for Standardization. *Natural gas - Online gas chromatograph for upstream*. Geneva, Switzerland: ISO; 2016.
- [27] Li F, Zhao Q, Sun C, Zhu L, Xia J, Huang B. Probing natural gas components with Raman integrating sphere technology. *Opt Lett* 2023;48:187. <https://doi.org/10.1364/ol.474494>.
- [28] Petrov DV, Matrosov II, Zaripov AR, Tanichev AS. Raman Natural Gas Analyzer: Effects of Composition on Measurement Precision. *Sensors* 2022;22. <https://doi.org/10.3390/s22093492>.
- [29] Torres LF, Damascena MA, Alves MMA, Santos KS, Franceschi E, Dariva C, et al. Use of near-infrared spectroscopy for the online monitoring of natural gas composition (hydrocarbons, water and CO<sub>2</sub> content) at high pressure. *Vib Spectrosc* 2024;131. <https://doi.org/10.1016/j.vibspec.2024.103653>.
- [30] Haghi RK, Yang J, Tohidi B. Fourier Transform Near-Infrared (FTNIR) Spectroscopy and Partial Least-Squares (PLS) Algorithm for monitoring Compositional changes in Hydrocarbon gases under in Situ pressure. *Energy Fuels* 2017;31:10245–59. <https://doi.org/10.1021/acs.energyfuels.7b01677>.
- [31] Eichmann SC, Kiefer J, Benz J, Kempf T, Leipertz A, Seeger T. Determination of gas composition in a biogas plant using a Raman-based sensorsystem. *Meas Sci Technol* 2014;25. <https://doi.org/10.1088/0957-0233/25/7/075503>.
- [32] Tanichev AS, Petrov DV. Raman Spectrum of Water Vapor in methane. *J Raman Spectrosc* 2025. <https://doi.org/10.1002/jrs.6813>.
- [33] Majumder D, Janani R, Scrimshire A, Stone A, Brooks W, Holcroft C, et al. Raman gas sensing technology: a new horizon? *Sens Actuators Rep* 2025;9. <https://doi.org/10.1016/j.snr.2025.100311>.
- [34] Maksimov P, Laari A, Ruuskanen V, Koironen T, Ahola J. Gas phase methanol synthesis with Raman spectroscopy for gas composition monitoring. *RSC Adv* 2020;10:23690–701. <https://doi.org/10.1039/d0ra04455e>.
- [35] International Organization for Standardization. *Natural gas-Upstream area-Determination of composition by Laser Raman spectroscopy*. Geneva, Switzerland: ISO; 2020.
- [36] Tanichev AS, Petrov DV. Simulation of v<sub>2</sub> Raman band of methane as a function of pressure. *J Raman Spectrosc* 2022;53:654–63. <https://doi.org/10.1002/jrs.6145>.
- [37] Van Aghoven MA, Fujisawa G, Rabbito P, Mullins OC. Near-infrared spectral analysis of gas mixtures. *Appl Spectrosc* 2002;56:593–8. <https://doi.org/10.1366/0003702021955376>.
- [38] Dąbrowski KM, Kuczyński S, Barbacki J, Włodek T, Smulski R, Nagy S. Downhole measurements and determination of natural gas composition using Raman spectroscopy. *J Nat Gas Sci Eng* 2019;65:25–31. <https://doi.org/10.1016/j.jngse.2019.02.003>.
- [39] Wang JL, Song ZH, Li LJ, Yang LL, Wang QY, Chou IM, et al. Integration of a fused silica capillary and in-situ Raman spectroscopy for investigating CO<sub>2</sub> solubility in n-dodecane at near-critical and supercritical conditions of CO<sub>2</sub>. *Pet Sci* 2022;19:3124–33. <https://doi.org/10.1016/j.petsci.2022.06.014>.
- [40] Takebayashi Y, Sagisaka M, Sue K, Yoda S, Hakuta Y, Furuya T. Near-infrared spectroscopic study of a water-in-supercritical CO<sub>2</sub> microemulsion as a function of the water content. *J Phys Chem B* 2011;115:6111–8. <https://doi.org/10.1021/jp201722f>.
- [41] Bharti SK, Roy R. Quantitative <sup>1</sup>H NMR spectroscopy. *TrAC* 2012;35:5–26. <https://doi.org/10.1016/j.trac.2012.02.007>.
- [42] McKenzie JS, Donarski JA, Wilson JC, Charlton AJ. Analysis of complex mixtures using high-resolution nuclear magnetic resonance spectroscopy and chemometrics. *Prog Nucl Magn Reson Spectrosc* 2011;59:336–59. <https://doi.org/10.1016/j.pnmrs.2011.04.003>.
- [43] Simmler C, Napolitano JG, McAlpine JB, Chen SN, Pauli GF. Universal quantitative NMR analysis of complex natural samples. *Curr Opin Biotechnol* 2014;25:51–9. <https://doi.org/10.1016/j.copbio.2013.08.004>.
- [44] Miller SL, Sartini M, Windom BC, Suiter CL, McLinden MO, Levinger NE, et al. High-pressure Vapor-Liquid Equilibrium Measurements of methane + Water Mixtures by Nuclear magnetic Resonance Spectroscopy. *Gas Sci Eng* 2023.
- [45] Duchowny A, Mohnke O, Thern H, Dupuy PM, Widerøe HC, Faanes A, et al. Composition analysis of natural gas by combined benchtop NMR spectroscopy and mechanical multivariate regression. *Energy Rep* 2022;8:3661–70. <https://doi.org/10.1016/j.egyr.2022.02.289>.
- [46] Duchowny A, Dupuy PM, Widerøe HC, Berg OJ, Faanes A, Paulsen A, et al. Versatile high-pressure gas apparatus for benchtop NMR: Design and selected applications. *J Magn Reson* 2021;329:107025. <https://doi.org/10.1016/j.jmr.2021.107025>.
- [47] Duchowny A, Ortiz Restrepo SA, Adams M, Thelen R, Adams A. Refined high-pressure tube design for improved resolution in high-pressure NMR spectroscopy. *Analyst* 2022;147:3827–32. <https://doi.org/10.1039/d2an00926a>.
- [48] Kamin Z, Bono A, Leong LY. Simulation and optimization of the utilization of triethylene glycol in a natural gas dehydration process. *Chem Prod Process Model* 2017;12:1–9. <https://doi.org/10.1515/cppm-2017-0017>.
- [49] Ortiz Restrepo SA, Swiatek A, Ohligschläger A, Mohnke O, Thern H. Quantitative composition analysis of natural gas by high-pressure proton low-field NMR Spectroscopy : development of an improved experimental methodology. *Gas Sci Eng* 2024;8026428.
- [50] Begum SK, Clarke RJ, Ahmed MS, Begum S, Saleh MA. Volumetric, viscosimetric and surface properties of aqueous solutions of triethylene glycol, tetraethylene glycol, and tetraethylene glycol dimethyl ether. *J Mol Liq* 2013;177:11–8. <https://doi.org/10.1016/j.molliq.2012.09.015>.
- [51] Kriesten E, Alsmeyer F, Bardow A, Marquardt W. Fully automated indirect hard modeling of mixture spectra. *Chemom Intel Lab Syst* 2008;91:181–93. <https://doi.org/10.1016/j.chemolab.2007.11.004>.
- [52] Zientek N, Laurain C, Meyer K, Kraume M, Guthausen G, Maiwald M. Simultaneous 19F-1H medium resolution NMR spectroscopy for online reaction monitoring. *J Magn Reson* 2014;249:53–62. <https://doi.org/10.1016/j.jmr.2014.10.007>.
- [53] Zientek N, Laurain C, Meyer K, Paul A, Engel D, Guthausen G, et al. Automated data evaluation and modelling of simultaneous 19F-1H medium-resolution NMR spectra for online reaction monitoring. *Magn Reson Chem* 2016;54:513–20. <https://doi.org/10.1002/mrc.4216>.
- [54] Sagmeister P, Lebl R, Castillo I, Rehl J, Krusz J, Sipek M, et al. Advanced real-time process analytics for multistep synthesis in continuous flow\*\*. *Angew Chem Int Ed* 2021;60:8139–48. <https://doi.org/10.1002/anie.202016007>.
- [55] Duchowny A, Ortiz Restrepo SA, Kern S, Adams A. Quantification of PVC plasticizer mixtures by compact proton NMR spectroscopy and indirect hard modelling. *Anal Chim Acta* 2022;1229:340384. <https://doi.org/10.1016/j.aca.2022.340384>.
- [56] Ortiz Restrepo SA, Adams A. Fast quantification of water content in glycols by compact 1H NMR spectroscopy. *Talanta* 2023;253:123973. <https://doi.org/10.1016/j.talanta.2022.123973>.

- [57] Babji NR, McCusker EO, Whiteker GT, Canturk B, Choy N, Creemer LC, et al. NMR chemical shifts of trace impurities: industrially preferred solvents used in process and green chemistry. *Org Process Res Dev* 2016;20:661–7. <https://doi.org/10.1021/acs.oprd.5b00417>.
- [58] Meyer K, Rademann K, Panne U, Maiwald M. Quantitative NMR spectroscopy for gas analysis for production of primary reference gas mixtures. *J Magn Reson* 2017; 275:1–10. <https://doi.org/10.1016/j.jmr.2016.11.016>.
- [59] Ortiz Restrepo SA, Denninger J, Adams M, Thelen R, Adams A. Composition analysis of hydrogen-enriched natural gas by high-pressure benchtop NMR spectroscopy with a low-cost flow-through cell design. *Int J Hydrogen Energy* 2024;66:604–11. <https://doi.org/10.1016/j.ijhydene.2024.04.119>.
- [60] Soininen P, Haarala J, Vepsäläinen J, Niemitz M, Laatikainen R. Strategies for organic impurity quantification by <sup>1</sup>H NMR spectroscopy: Constrained total-line-shape fitting. *Anal Chim Acta* 2005;542:178–85. <https://doi.org/10.1016/j.aca.2005.03.060>.
- [61] Suiter CL, McLinden MO, Bruno TJ, Widegren JA. Composition determination of low-pressure gas-phase mixtures by <sup>1</sup>H NMR Spectroscopy. *Anal Chem* 2019;91: 4429–35. <https://doi.org/10.1021/acs.analchem.8b04955>.
- [62] Hall AMR, Chouler JC, Codina A, Gierth PT, Lowe JP, Hintermair U. Practical aspects of real-time reaction monitoring using multi-nuclear high resolution FlowNMR spectroscopy. *Cat Sci Technol* 2016;6:8406–17. <https://doi.org/10.1039/c6cy01754a>.
- [63] Giraudeau P, Felpin FX. Flow reactors integrated with in-line monitoring using benchtop NMR spectroscopy. *React Chem Eng* 2018;3:399–413. <https://doi.org/10.1039/c8re00083b>.
- [64] Ratel G. Evaluation of the uncertainty of the degree of equivalence. *Metrologia* 2005;42:140–4. <https://doi.org/10.1088/0026-1394/42/2/009>.